A study of the sedimentation of noncolloidal bidisperse, concentrated suspensions by an acoustic technique

M. Hoyos
Laboratoire de Physique et Mécanique de Milieux Hétérogènes, Ecole Supérieure de Physique et Chimie Industrielles de la Ville de Paris 10, rue Vauquelin, 75232 Paris, Cedex 05, France

J. C. Bacri, J. Martin, and D. Salin
Laboratoire Acoustique et Optique de la Matière Condensée, Université Pierre et Marie Curie Case 78, 4 Place Jussieu, 75252 Paris Cedex 05, France

(Received 11 November 1992; accepted 1 August 1994)

This paper uses an acoustic technique to determine the concentration profile developing during the sedimentation of noncolloidal bidisperse suspensions of glass beads in a Newtonian fluid. Various bead diameter ratios have been used and a wide range of relative concentrations is covered. From the shock front velocities and the concentrations in different zones, the sedimentation velocities of small and large particles in a homogeneous suspension of respective concentrations c_{s0} and c_{l0} have been determined. The semidilute regime ($c_0=s_{s0}+c_{l0}<20\%$) has many similarities with the dilute regime, where large particles provide the dominant hydrodynamic hindrance to settling. In the concentrated regime ($c_0>35\%$), a mutual hindrance leads to a velocity reduction of large particles and to an enhancement of small ones, as compared to a monodisperse suspension. The data clearly demonstrate that size segregation in the concentrated regime disappears at a critical concentration, which for the size ratio 1.68 is equal to $c_0=45\%$. © *1994 American Institute of Physics.*

I. INTRODUCTION

Sedimentation is a process widely used in the industry as a method for size determination, fractionation of powders, separation, such as photosedimentation, and segregation. Because of the complex nature of the hydrodynamic and physicochemical phenomena governing particle–particle and fluid–particle interactions, sedimentation of suspensions or of fluidized beds represents a broad subject. Useful studies of this complex process rely on model systems, such as mono- or bidisperse suspensions of spherical particles. To interpret experiments[1] of the sedimentation of monodisperse dispersions, different approaches of both dilute[2] and concentrated[3–9] regimes have been successfully developed. With the exception of the very dilute limit,[10–14] however, noncolloidal (but also colloidal) bidisperse suspensions still represent a theoretical challenge. Early experiments[12–20] have clearly established the salient features of the bidisperse problem. Searching for size separation, Davies[17] observed size segregation of concentrated suspensions up to a critical concentration, above which particle interlocking prevented further segregation, and the bidisperse suspension falls *en masse*. It was found that the smaller the ratio of the large to small particle diameters, the smaller the critical concentration. Effects of polydispersity were also analyzed.

A tentative modeling of these features has also been attempted. Withmore[16] considered the problem of differential settling of a mixture of particles of two different sizes using an extension of the cell model developed by Happel[5] for the study of particle interactions in a monodisperse concentrated suspension. Lockett and Al-Habbooby,[18] Mirza and Richardson,[19] Selim *et al.*,[20] and Al-Naafa and Selim[14] proposed expressions for the sedimentation velocities of the large size, $v_l(c_{s0},c_{l0})$, and the small size; $v_s(c_{s0},c_{l0})$, particles in an homogeneous suspension of respective concentrations c_{s0} and c_{l0}, by extending the phenomenological relation of Richardson and Zaki[4] for monodisperse suspensions. These velocities are determined from the total voidage $c_0=c_{s0}+c_{l0}$. Unfortunately, these models completely miss the nonsymmetric character of the hydrodynamic interaction between large and small particles.[2] Nonetheless, due mostly to the large number of adjustable parameters and the limited accuracy of the measurements, the predicted sedimentation front velocities appear to be in reasonable agreement with measurements. In fact, this model has lead to the conclusion that segregation would always occurs,[19] which is in contradiction with some experiments.[4,15,17,20] A more complete theory concerning polydisperse concentrated suspensions was developed by Mazur and Van Saarlos,[6] although only hydrodynamic interactions were considered with no application to batch sedimentation developed, thus the model cannot be used for comparison with experiments.

Although the salient features of concentrated bidisperse suspensions have been observed[17] more experiments are needed to provide accurate data for a critical test of the various theories. This issue has been successfully addressed in the dilute limit.[10,14] For larger concentrations, the desirable technique must be able to give the concentration evolution of both large and small spheres along the sedimentation axis. In either regime the sedimentation scenario is indeed very simple: two shock fronts are generally observed, one be-

 1070-6631/94/6(12)/3809/9/$6.00

tween the clear fluid and the small particles, the other between the small particles and a homogeneous suspension of small and large particles. In previous experiments[14–20] the velocities of these two fronts, but not the particle concentrations have been measured using colored particles. More recently, concentration profiles along the sedimentation column have been determined with techniques based on transmission (or backscattering) of light,[12] x rays,[13] and even NMR.[21] However, these transparency-based techniques become insufficiently accurate at concentrations larger than 15%, hence only dilute and semidilute suspensions have been investigated. Furthermore, most of these experimental equations results give shock front velocities instead of the sedimentation velocity of each species and with the exception of Davies,[17] the question of segregation occurrence was not directly addressed. Determination of concentration profiles of concentrated suspensions requires a different tool. A promising technique in this direction is based on acoustics[22] where the concentration is derived from sound of speed variations. This method was originally developed for the analysis of fluid flow in porous media.[23,24] It has proved to be powerful for studying noncolloidal monodisperse suspensions, particularly at high concentration.[25] It must be pointed out that in the acoustic technique, the larger the concentration, the more accurate the measurements.

In this paper we present an experimental study on batch sedimentation of noncolloidal bidisperse suspensions of spheres of equal density. The objectives of this study are to provide data suitable for a subsequent theoretical model, namely data on the sedimentation velocities of small and large particles in a homogeneous suspension of concentration, and to track the boundaries of occurrence of the segregation process. For this purpose, we focus on the semidilute-to-concentrated range (15%–45%) which has not yet been covered, and in which our technique is decisively useful. This concentration range has the advantage of being less affected by the natural residual polydispersity of the spheres of species,[21,26,27] while it also leads to the possibility of segregation inhibition.[17] The size-ratio range studied is between 1.15 to 3.9 with a wide range of relative concentration of each species being covered (5%–40% to 25%–40%). From the measurements we determine two sedimentation velocities, those of the large particles and of the small particles in a mixture of the two and compare the corresponding hindered settling functions to the monodisperse case, focusing on the reduction, and eventually the loss of segregation at high concentrations.

II. BIDISPERSE SUSPENSION SEDIMENTATION

The basic theory of suspension sedimentation was developed by Kynch[3] and has been used to describe experiments on both mono- and bidisperse suspensions.[1,12–16,19,20,25–27] In a monodisperse suspension of volume fraction c, the sedimentation profile is determined from the concentration dependence of the particle settling velocity, $v(c)$, as follows from Kynch's theory.[3] First, from $v(c)$ one obtains the particle flux $cv(c)$. Then, for a given initial concentration c_0, the concentration profile $c(z,t)$ in the sedimentation column is determined from the solid–particle conservation equation.

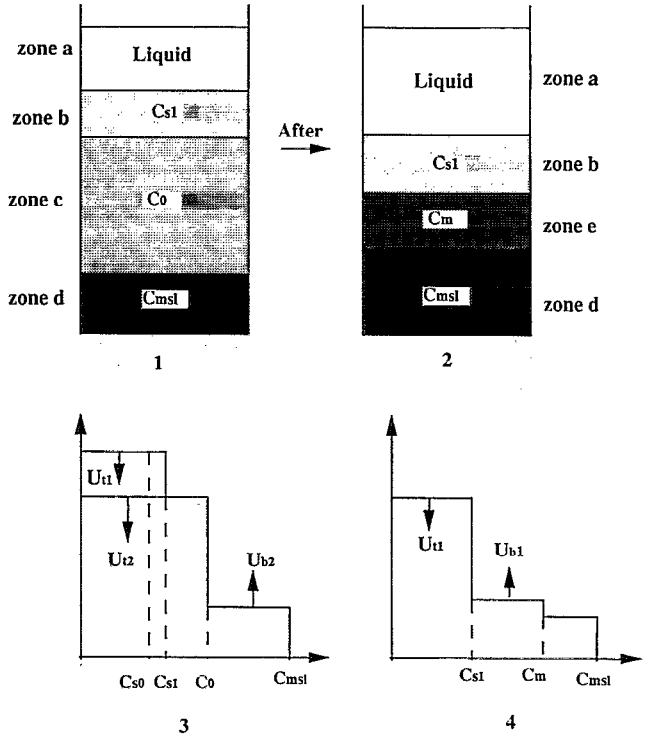

FIG. 1. Sedimentation of a bidisperse suspension. Top (1 and 2) shows schematic of the different concentration zones in the column; bottom (3 and 4) shows, corresponding shock fronts. The following zones exist: (a) clear fluid, (b) small particles at the enhanced concentration $c_{s1}>c_{s0}$ (c), small and large particles at their respective initial concentration, c_{s0} and c_{l0} ($c_0=c_{s0}+c_{l0}$), (d) sediment of small and large particles at concentration c_{msl}. After sedimentation we get the situation at right (2 and 4), in which zone c has disappeared whereas the sediment builds up from only small particles leading to a sediment concentration c_m.

In a bidisperse suspension of initial concentrations c_{s0} and c_{l0} of small and large particles, respectively, the sedimentation profile observed consists of four homogeneous zones (Fig. 1-1). From top to bottom we distinguish the following.

Zone a: A top zone of clear fluid ($c=0$).

Zone b: A second zone consisting of a suspension of small particles only, of a concentration higher than the initial, c_{s0}. This enhanced concentration we will call c_{s1}.

Zone c: A third zone, where we find particles of both sizes at the initial concentrations c_{s0} and c_{l0}.

Zone d: Finally a fourth zone, where we find the sediment of particles of both sizes in the first stage of sedimentation. Later on (Fig. 1-2), when all large particles have settled, a further layer grows on the sediment containing only small particles (zone e). We remark that in zone d, where the sediment is composed of both species, the packing concentration is higher than that in zone e composed of only one species.

These zones are of variable extent and they are separated by three shock fronts propagating at different velocities (Fig. 1-3): two fronts propagate from top to bottom with velocities U_{t1} and U_{t2}, respectively, and one from bottom to top with velocity U_{b2}. Later on (Fig. 1-4), only one from the top (U_{tl}) and one from the bottom (U_{b1}). These fronts are of course

broadened by hydrodynamic dispersion, but their propagating velocity remains the same.[26,28]

Such a concentration profile with three shock fronts is a consequence, through Kynch theory, of the concentration dependence of the settling velocity of the small and large particles, $v_s(c_s,c_l)$ and $v_l(c_s,c_l)$, respectively, which we wish to determine. In our acoustic experiments we can measure the total concentration (c_s+c_l) along the sedimentation column in each zone. The conservation of each species of particles given appropriate relationships between shock fronts and settling velocities as follows.

(1) For the top front between the clear fluid (where, $c_s=c_1=0$) and zone b (where the small particles have a measured concentration c_{s1}) we have

$$U_{t1}=v_s(c_{s1},0). \tag{1}$$

(2) For the second top front between the small particles zone b $(c_{s1},0)$ and the mixture zone c (c_{s0},c_{l0}) we have

$$U_{t2}=\frac{c_{s1}v_s(c_{s1},0)-c_{s0}v_s(c_{s0},c_{l0})}{c_{s1}-c_{s0}}, \tag{2}$$

$$U_{t2}=v_l(c_{s0},c_{l0}). \tag{3}$$

Note that the concentration of the particles in zone b must be larger than that in zone c, $c_{s1}>c_{s0}$, in order to satisfy Eqs. (2) and (3) simultaneously leading to the enhanced concentration effect in zone b. This experimentally observed scenario is quite simple, although more complicated behavior can occur even for monodisperse suspensions (3). To summarize, the shock front velocities, U_{t1} and U_{t2} lead to the following: (i) The monodisperse sedimentation velocity $v_s(c_{s1},0)$, where c_{s1} has to be determined acoustically. Note that in previous experiments[14–20] the determination of c_{s1} is not made, relying instead on monodisperse sedimentation velocity, from Eq. (1). (ii) The large size particle sedimentation velocity in presence of both small and large particles, $v_l(c_{s0},c_{l0})$, from Eq. (3). (iii) the sedimentation velocity of the small-size particle in a homogeneous suspension of small and large ones, by combining Eqs. (1) and (2):

$$v_s(c_{s0},c_{l0})=U_{t2}-(U_{t2}-U_{t1})c_{s1}/c_{s0}. \tag{4}$$

The functional dependence of the two velocities, $v_s(c_{s0},c_{l0})$ and $v_l(c_{s0},c_{l0})$ is desirable to test theoretical predictions on bidisperse suspensions. More precisely, more convenient for comparison are the hindrance functions $v_s(c_{s0},c_{l0})/v_s^0$ and $v_l(c_{s0},c_{l0})/v_l^0$, where $v_s^0(v_l^0)$ are the settling velocities of small (large) single particle (Stokes velocity). From Richardson and Zaki (4) correlation, a large amount of effort has been devoted to try to fit the entire range of the monodisperse settling hindrance with a power-law function of the voltage, i.e., $(1-c)^n$, where the exponent depends on the Reynolds number (or the Péclet number in the case of colloidal suspensions). For lack of measurement of c_{s1}, such a correlation is generally used[14–20] for bidisperse suspensions. The failure of this fit procedure instead of the real measured value appears when the two terms of the right-hand side (RHS) of Eq. (4) are of the same order of magnitude, i.e., in the vicinity of the inhibition of the segregation process.

III. EXPERIMENTS

The acoustic technique to be used has proved useful in the study of monodisperse concentrated sedimenting suspensions.[22,25] The use of the technique for bidisperse systems is a second thrust of this effort. We recall that the speed of sound in suspensions is related to the volume fraction of particles, hence the sedimentation profile can be determined by measuring variations in the sound speed at several cross sections along the sedimentation column.[25] Acoustic techniques for determining the local concentration are not widely used, although we believe them to be quite useful for the study of suspension and fluidized beds: we shall proceed with a brief description of the main outlines of acoustics.[22]

A. Acoustics of suspensions

There are two main measurable quantities, the sound speed and the attenuation of the sound wave. The former is linked to the elasticity and the density of the medium the latter reflects the dissipation mechanism (viscous, inertia,...). While the particular problem of suspensions deserves specific approaches,[29] it can generally be included in the theory of propagation of sound in porous media developed 35 years ago by Biot.[30] In this continuum theory (where the sound wavelengths are much larger than the bead size a) and for inertia-dominated regimes (high-frequency regime),[30,31] the sound speed is given by expressions

$$V=\sqrt{K/\rho}, \tag{5}$$

where

$$K^{-1}=cK_s^{-1}+(1-c)K_f^{-1}$$

and

$$\rho=\alpha\rho_f\frac{c\rho_s+(1-\alpha^{-1})(1-c)\rho_f}{c(1-c)\rho_s+(\alpha-1+c^2)\rho_f}.$$

Here, K_s, K_f, ρ_s, ρ_r denote the compressibilities and densities of solid and fluid, respectively, c is the suspension concentration and $\alpha=1+c/2(1-c)$ is the tortuosity which characterizes the inertia coupling between solid and fluid. As is evident from Eq. (5), the sound speed is concentration dependent. In Fig. 2 we show measurements of the sound speed as a function of the concentration of 33–44 μm glass beads in silicon oil suspension. The solid line is the theoretical formula [Eq. (5)]. In the frequency range used (350 kHz, wavelength ~3 mm), the sound speed is mainly insensitive to the bead size but the attenuation does depend on it.[31] At a higher frequency (~5 MHz) scattering becomes important for a ~50 μm and Biot's theory no longer applies.[35] From the calibration curve (Fig. 2) we can deduce that a concentration variation of 0.1% yields a relative variation in sound speed of $5\,10^{-5}$ in the vicinity of $c=0$, and of $5\,10^{-4}$ in the vicinity of $c=50\%$. An accuracy in c of 0.1% on the whole range requires an accuracy of 5×10^{-5} in relative sound speed measurements. Hence, as opposed to other techniques (x rays, NMR or light scattering), the larger the concentration the better would be the accuracy of our measurements.

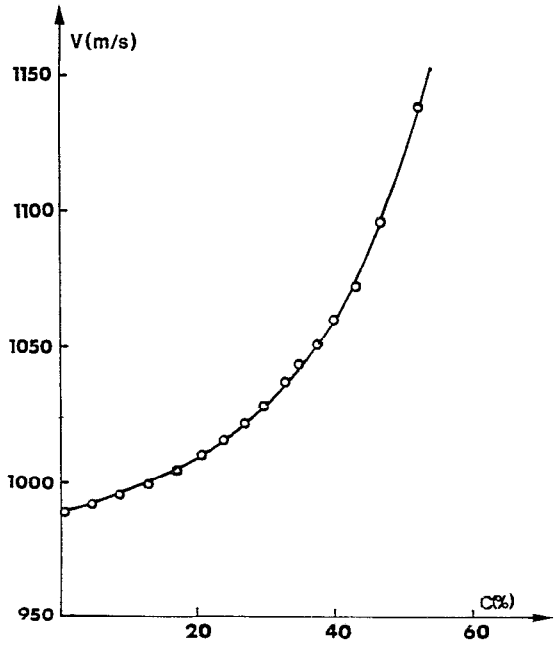

FIG. 2. Sound velocity versus concentration of a 37–44 μm glass bead suspension in silicone oil (frequency 350 kHz). The line through the data is the theoretical prediction [Eq. (5)].

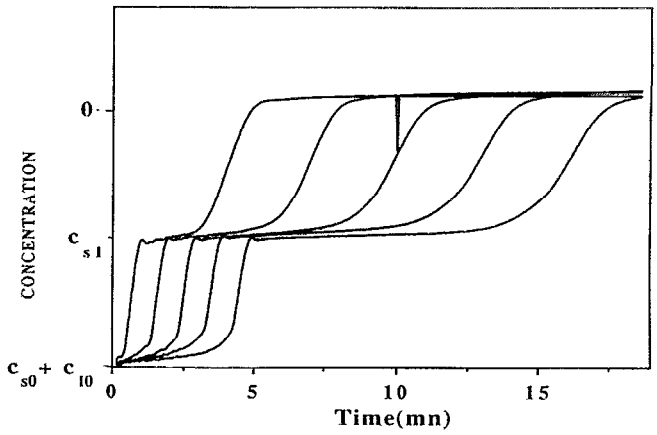

FIG. 4. Concentration profiles versus time at five equidistant heights in the sedimentation column for a bidisperse suspension. The two shock fronts propagate downwards at constant velocities U_{t1} and U_{t2} (top fronts of Fig. 1).

B. Sound speed variation measurements

To accurately measure sound velocity variations, we have designed an automated system, the principle of which is sketched in Fig. 3. The key element of the system is the transducer probe. It consists of uniformly spaced zirconate titanate (PZT) elements which have been sawed and polished. Each PZT element is 5.6 mm wide, 10 mm long, and 2 mm thick. Thus the resonance frequency is of the order of 350 kHz. The bandwidth is quite narrow because there is no damped backing. This has the definite advantage of increased its sensitivity. The 350 kHz frequency used is both high enough to lead a good time resolution and low enough to avoid scattering attenuation. A pulse function generator (Exact 628) sends an electrical sine pulse (15 V peak to peak) to the transmitting transducer at a 350 kHz frequency; this pulse is received by the opposite transducer after a time of flight τ. The received signal, which has been attenuated due to the acoustic mismatch at the successive interfaces (transducer/boundary/suspension) and due to diffraction and acoustic attenuation in the different media is electronically amplified (60 dB). Changes in the fluid concentration inside the suspension induce sound velocity variations, hence variations of the time of flight τ. The experiments on bidisperse suspensions are performed in a 30 cm high sedimentation column of rectangular cross section 4×3 cm^2. The epoxy boundaries (sound speed $\sim$2000 m/s) are 1 cm thick. The overall time of flight is then of the order of 40 μs (30 μs from the suspension). This τ value is precisely measured by a counter timer (Racal Dana 1990 Universal Counter) with an accuracy of better than 0.01 ns. All these equipments are computer-controlled (Hewlett Packard Vectra Q5/16). The accuracy in τ measurements is limited by the electronic fluctuations of the signal. A typical signal received has a voltage $U=500$ mV with noisy fluctuations $\delta U=10$ mV leading, over a quarter period $T/4=700$ ns, to fluctuations $\delta\tau=15$ ns and a relative accuracy in τ, i.e., in sound velocity, of 5×10^{-4}. To get the desired 5×10^{-5} accuracy, the signal is averaged over at least 100 cycles, with a repetition rate of the transmitted pulse of 1 ms, a measurement of the desired accuracy 5×10^{-5} is achieved in 0.1 s. The spatial resolution is typically 3 mm in the direction of sound propagation, close to the 2 mm transducer thickness. Concentration measurements are achieved by means of ten pairs of transmitter–receiver piezoelectric transducers laid along z, the height side of the column. In our device (Fig. 4), the transducer positions are fixed and we record automatically the sound velocity variations as a function of the time.

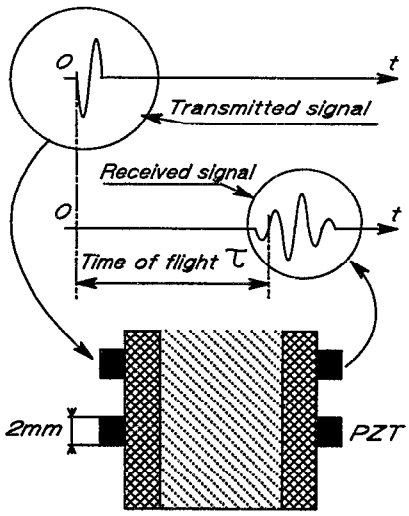

FIG. 3. Experimental device.

TABLE I. Characteristics of the bidisperse suspensions.

Mixture n^0	a_s (μm)	a_l (μm)	$\lambda=a_l/a_s$	η (cp)
1	37–44	74–88	2	6
2	37–44	105–125	2.83	6
3	37–44	149–177	3.91	6–10
4	63–74	105–125	1.68	6
5	63–74	74–88	1.19	6

C. Suspensions

The suspensions consist of binary mixtures of several sizes of glass beads of density 2.42 g/cm^3, dispersed in a sucrose–water solution (Newtonian fluid). Table I gives the different binary mixtures and liquid viscosities used. The given range of particle diameters corresponds to 95% of the particle fraction. Then the mean diameter a is half the sum of the two extremes values. Because the difference between these values is four times the width σ of their Gaussian distribution function, then, $\sigma/a \sim 5\%$. In all suspensions studied, the Reynolds number is smaller than 0.001, leading to negligible inertia corrections, while the Péclet number is always larger than 1000 leading to negligible Brownian effects.[25] Experiments were carried out by adding the weighed liquid and a mixture of glass beads to the column; triton $\times 100$, is used to avoid aggregation of particles. The system is kept at a constant temperature (23 ± 0.1 °C). A rectangular plunger is used to mix the suspension. Shaking and mixing the suspension is important in the experimental procedure in order to obtain a uniform initial bulk concentration throughout the column. Our acoustic device allows us to test the homogeneity of the concentration with an accuracy better than 0.1%. As sound velocity (mainly in fluids) is temperature dependent the acoustics also allows to test the thermal uniformity before the onset of the experiments. When the suspension is mixed homogeneously, the time evolution of the sound velocity is recorded for different heights in the sample, leading to the concentration profile $c(z,t)$.

The various mixtures are prepared as follows: first, we introduce small particles at the given concentration c_{s0} in the column containing the liquid; then, large particles are added in steps of 2%. Experiments were performed up to a total concentration of 45%. Larger concentrations lead to difficulty in creating a homogeneous suspension because stirring is not effective. About 150 experiments were carried out for different mixtures and at different volume fractions.

IV. RESULTS AND DISCUSSION

Typical examples of experimental concentration profiles are shown in Fig. 4 for a bidisperse suspension ($a_s=68$ μm, $a_l=115$ μm, $c_{s0}=15\%$, $c_{l0}=17\%$). We show five typical profiles, at various locations in the sedimentation column ($z=4.5$, 6, 7.5, 9, 10.5 cm from the top of the suspension). Each curve, corresponding to a transducer location, gives as a function of time, the time of flight variations of a sound wave through the suspension, hence the local concentration. The curves look continuous because of the large amount of data. Each profile exhibits simple concentration changes

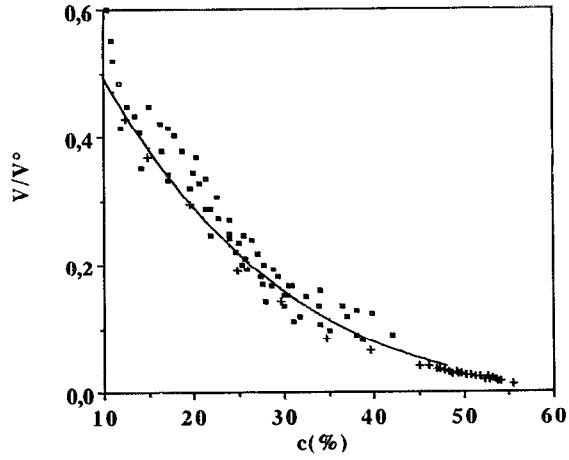

FIG. 5. Normalized settling velocity of the top front, $v_s(c_{s1})/v_s$ versus c_{s1}, the enhanced concentration. Data sets correspond to various initial concentrations $c_{s0}=15\%$, 20%, 25% (full squares). The crosses are the monodisperse normalized settling velocity measured previously (25). The line is a best-fit guide line.

(within the natural width of our acoustic device[25]) corresponding to the shock fronts described earlier. However, these shock fronts are regularly spaced; proving that they propagate at constant velocities, although a more careful inspection of the profile shows a small spreading of the front as time goes on. This spreading is due to two well-known phenomena, namely residual polydispersity and hydrodynamic dispersion;[12,21,26–28] the former leads to a spreading proportional to time, the latter to a spreading proportional to the square root-of-time. It has been experimentally observed[21,26] that polydispersity eventually overcomes dispersion and that the larger the concentration the smaller is the polydispersity spreading. In our experiments, where we are concerned with semidilute-to-concentrated suspensions, we define the shock-front velocities at the half-concentration of the corresponding front (as in Ref. 12) and we measure its value after some time has elapsed. As anticipated from Sec. II, in Fig. 4 there are two shock fronts which occur successively, with respective velocities U_{t1} and U_{t2}. These fronts separate the homogeneous initial suspension (c_{s0}, c_{l0}) the monodisperse suspension (c_{s1},0) and the clear fluid (0,0). As discussed previously, from these experimental data, we can extract U_{t1}, U_{t2}, and c_{s1} in zone b (Fig. 1-1). At this stage, the fact that zone b consists of the small size particles is only a guess. We test this conjecture in Fig. 5, where we plot the hindered settling velocities, i.e., $v_s(c_{s1},0)/v_s^0[v_s^0=v_s(0,0)]$ versus c_{s1} (where the Stokes settling velocity, v_s^0 is computed based on the mean particle diameter). The line through the data is a best fit, a power law with a correlation coefficient of 93%. Comparison with our measurements in a monodisperse suspension[25] (shown by crosses in Fig. 5) are in reasonable agreement with the theoretical predictions.[32,33] Figure 5 addresses questions of accuracy and reproducibility in our measurements; the concentration is accurately measured but there is a lack of reproducibility due to uncertainties of the stirring in each experiment, even when handled with care. Nonetheless, a statistical trend can clearly be inferred, and so

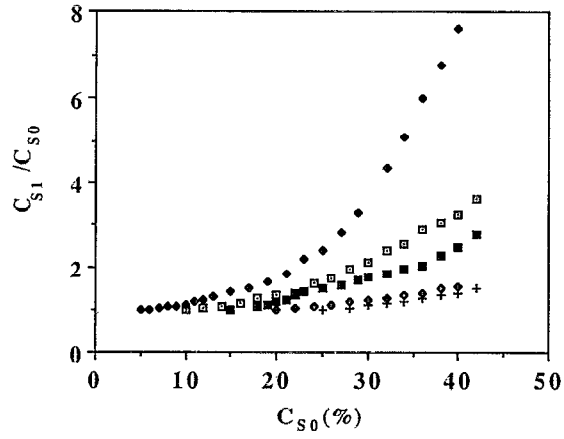

FIG. 6. Relative enhanced concentration of small particles, c_{s1}/c_{s0}, in zone b (Fig. 1), versus total concentration $c_0=c_{s0}+c_{l0}$. In each data set c_{s0} is kept constant whereas c_{l0} increases. $c_{s0}=5\%$ (◆), $c_{s0}=10\%$ (□), $c_{s0}=15\%$ (■), $c_{s0}=20\%$ (◇), $c_s=25\%$ (+).

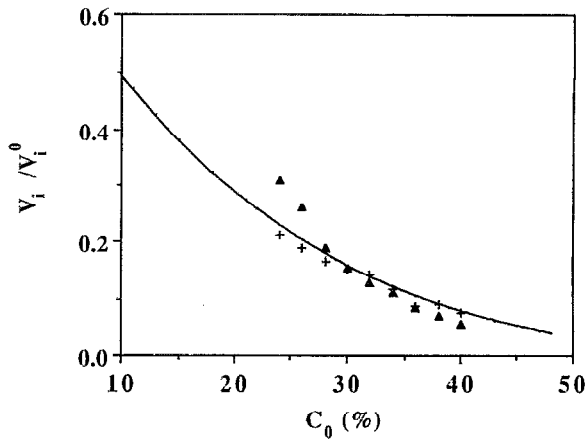

FIG. 8. As in Fig. 7, Normalized sedimentation velocities, for $\lambda=1.68$ and $c_{s0}=20\%$.

can the error bounds of each experiment, where we use the measured velocity (not the fit line which is just a guideline). This is also the case for Figs. 6–12. Regarding the statement that the top front consist of small beads, this hypothesis is consistent with the sedimentation scenario of Sec. II. Thus, from the experimental data (c_{s1},U_{t1},U_{t2}) we can derive the functional relations $v_1(c_{s0},c_{l0})$ [Eq. (3)] and $v_s(c_{s0},c_{l0})$ [Eq. (4)].

A. Enhanced concentration: ($c_{s1}>c_{s0}$)

Figure 6 is a plot of the relative concentration c_{s1}/c_{s0} of the small size particles in zone b (Fig. 1-1) against the total initial concentration $c_0=c_{s0}+c_{l0}$, for various initial concentrations of the small particles $c_{s0}=5$, 10, 15, 20, and 25%. Here, the particle mean sizes are $a_s=68$ μm and $a_l=115$ μm respectively, so that $\lambda=a_l/a_s=1.68$ (mixture number 4 in Table I). For each initial value c_{s0}, the ratio c_{s1}/c_{s0} steadily increases from 1 onwards as the initial large particles concentration, c_{l0}, increases. This conclusively proves and confirms[12–20] an enhanced concentration effect in zone b due to the increasing backflow from the large particles affecting the small ones in zone c, where small size particles are rejected towards zone b $(c_{s1},0)$ through the shock front, we note that the smaller the initial value c_{s0} the larger this effect. This determination of the concentration enhancement, c_{s1}/c_{s0}, is needed for the determination of $v_s(c_{s0},c_{l0})$ through Eq. (4).

B. Sedimentation velocities $v_s(c_{s0},c_{l0})$ and $v_l(c_{s0},c_{l0})$

Our data allows the determination of the sedimentation velocities $v_s(c_{s0},c_{l0})$ and $v_l(c_{s0},c_{l0})$ for different initial total concentrations, c_0, and for small particles concentrations c_{s0} for the binary mixtures given in Table I. Most authors[14–20] express $v_l(c_{s0},c_{l0})$, but also $v_s(c_{s1})$, obtained from U_{t1}, in terms of c_0 only. This is a misleading representation because $v_s(c_{s1})$ is not a unique function of c_0, different values of c_{s0} and c_{l0} with the same c_0 lead to different values of c_{s1}, hence of $v_s(c_{s1})$. In order to present the results in a form suitable for comparison with different sizes and with the monodisperse case, we normalized the data with the Stokes settling velocity of the isolated particles, as de-

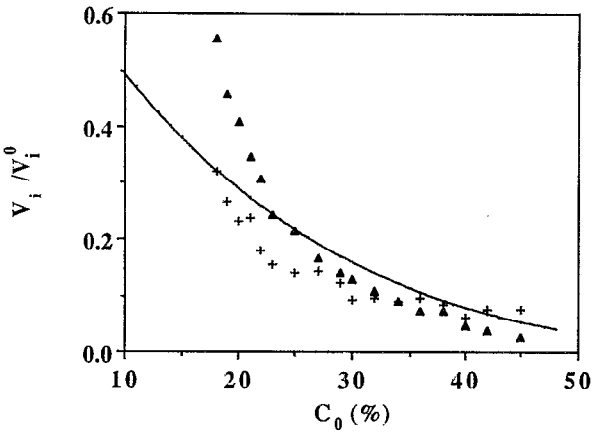

FIG. 7. Normalized sedimentation velocities (hindered settling functions) of small particles (+) $v_s(c_{s0},c_{l0})/v_s^0$ and large particles (▲) $v_l(c_{s0},c_{l0})/v_l^0$ versus total concentration $c_0=c_{s0}+c_{l0}$, for $\lambda=1.68$ and $c_{s0}=15\%$. The dashed line is the monodisperse hindered setting function, as in Fig. 5.

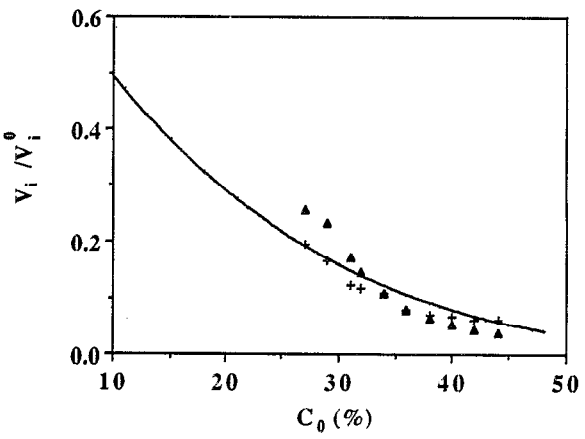

FIG. 9. Normalized sedimentation velocities, for $\lambda=1.68$ and $c_{s0}=25\%$.

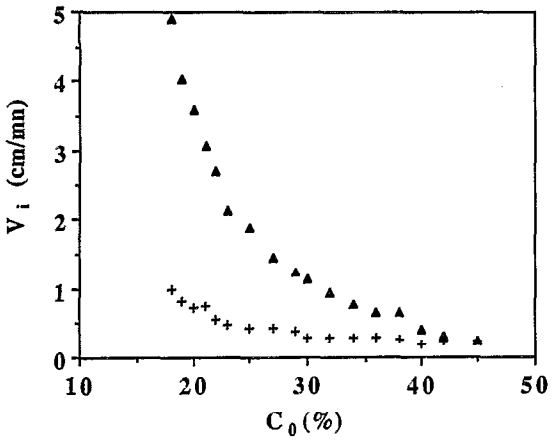

FIG. 10. Absolute sedimentation velocities, $v_s(c_{s0},c_{l0})$ (+) and $v_l(c_{s0},c_{l0})$ (▲) for $\lambda=1.68$ and $c_{s0}=15\%$. Note the convergence at $c_0=45\%$ of the two velocity series.

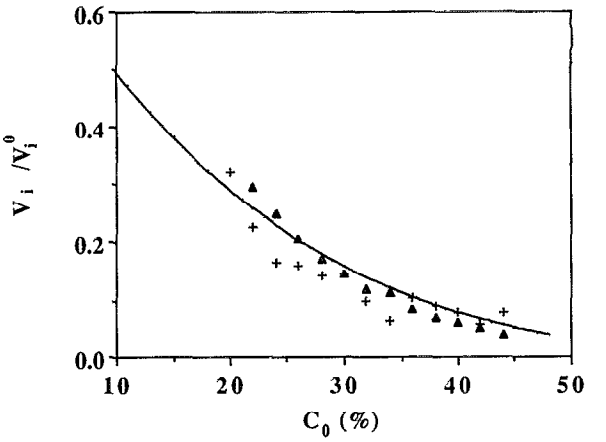

FIG. 12. Normalized sedimentation velocities for $\lambda=2.83$ and $c_{s0}=20\%$.

scribed previously. Figures 7–9 and 12 show the corresponding hindered settling functions $v_i(c_{s0},c_{l0})/v_i^0$ vs $c_0=c_{s0}+c_{l0}$, as well as the curve for the monodisperse suspensions given in Fig. 5.

In the analysis of our results, we will focus particularly on mixture number 4 ($c_{s0}=15$, 20, 25%, $a_s=68$ μm, $a_l=115$ μm, $\lambda=1.68$) because of its interesting behavior (Figs. 7–9). The following points can be noticed in Figs. 7–9.

(1) A comparison of the relative positions reveals a change in the three hindered settling functions from the low ($c_0<20\%$) to the high ($c_0>40\%$) concentration regime. In the semidilute regime the hindered function of the large particles is larger than that of the small particles. In contrast, in the concentrated regime it is exactly the opposite. In either regime, the monodisperse hindered settling function is more or less in between, crossing both curves at around 35%.

(2) At low concentrations, the velocity $v_l(c_{s0},c_{l0})$ of large particles settling among a mixture of large and small particles is larger than the velocity of the same size particles sedimenting in a monodisperse suspension at the same concentration c_0. While, the velocity $v_s(c_{s0},c_{l0})$ of the small particles is smaller than the sedimentation velocity of the same size for the monodisperse case at the same total concentration c_0. This regime must be viewed as an extension of the dilute regime[12,13] in which the hydrodynamic interactions follows the dilute theoretical predictions small particles hinder the large ones much less effectively than large ones hinder themselves, and large particles hinder the sedimentation of small particles more effectively than small ones hinder themselves.

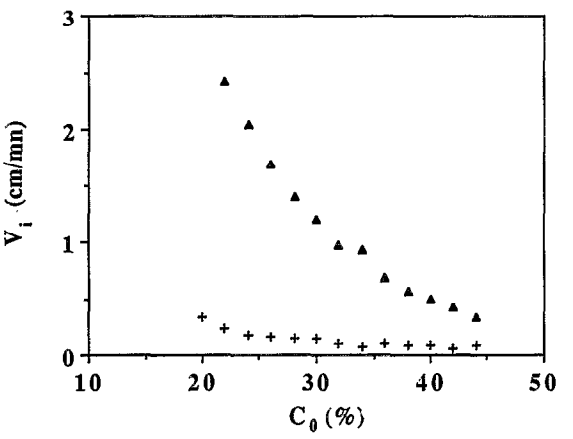

FIG. 11. Absolute sedimentation velocities for $\lambda=2.83$ and $c_{s0}=20\%$.

(3) At larger concentrations ($c_0>35\%$), however, we observe the opposite: the large particles settling velocity is smaller than the sedimentation velocity of a monodisperse suspension of large particles at the same concentration c_0, while the small particles settling velocity is larger than the sedimentation velocity of the monodisperse suspension also at the same c_0. This effect can be understood as a steric effect at high concentration, particles become interlocked and to overtake each other, large and small particles have to deal with geometric limitations. To accommodate this steric effect, large particles slow down whereas small ones are partially dragged along. We note that even though the hindered curve of the small particles lies above that of the large particles, the absolute velocity $v_l(c_{s0},c_{l0})$ is still larger than (or at least equal to) $v_s(c_{s0},c_{l0})$ (Fig. 10).

(4) As the concentration increases, the mutual obstruction of large and small particles keeps increasing leading to a removal of the segregation process, already observed (17). For most initial values c_{s0}, the two velocities, $v_s(c_{s0},c_{l0})$ and $v_l(c_{s0},c_{l0})$, of mixture number 4 converge to the same value at a large bulk volume fraction, c_I. This effect is demonstrated in Fig. 10 where the two settling velocities are presented in absolute values. At the critical concentration $c_I=c_0=45\%$, it has not been possible to separate the two species, even for a 1 m long column, we observe a single top front all along the column. The hindered functions of Figs. 7–9 show that the absolute velocity of the two species at the segregation concentration c_I is in between the monodisperse large and small settling velocities. For this particle size ratio ($\lambda=1.68$), segregation disappears at $c_I=45\%$ for an initial concentration, $c_{s0}=15\%$; for different initial small particle concentrations $c_{s0}=20$ and 25% (Figs. 8 and 9) this tendency is also observed eventually, although for slightly higher c_I

values. For smaller initial values c_{s0}=5, 10%, however, the segregation seems to persist for higher concentrations. The limiting concentration c_I is also the upper bound of concentration c_{sl} as c_0 varies, as depicted in Fig. 6 (where for, c_{s0}=15%, the ratio c_{s1}/c_{s0} tends to 3, i.e., c_{s1}=45% for $c_0=c_I$=45%). An important asset of our acoustic technique is its ability to measure with a high accuracy up to the vicinity of packing concentration, the value of the concentration c_{s1} in the upper zone, leading to $v_s(c_{s0},c_{l0})$. Thus, two different measurements give us the concentration at which segregation vanishes. Phenomenologically, we can think of this limiting concentration as that at which the particles become interlocked so that the small particles cannot pass through the interstitial spacing between the large particles and vice versa. Modeling this effect is still in progress.

C. Effect of size ratio λ

Experiments were also performed to see how the segregation inhibition depends on the particle size ratio λ.

(i) For λ=2.83 (mixture number 2), we observe the two shock fronts for all initial concentrations c_0, with the same proportions of c_{s0} and c_{l0} used previously for mixture 4. The data plotted in Fig. 11 (absolute velocities) show that there is no convergence of the velocities at high concentrations and segregation always occurs for this particular λ value. The corresponding hindered settling functions (Fig. 12) show a semidilute regime extending up to c_0=35% and a high concentrated regime (c_0>40%) in which large particles slow down and small ones are dragged along. This suggest that higher concentration might have led to segregation inhibition. Complementary experiments for λ=3.91 reinforce the same trends: the semidilute regime now extends almost over the entire range of concentration (up to 45%), the hindered settling function of large particles being always larger than that of small particles and very close to the monodisperse function. Thus, at this size ratio, large particles ignore the presence of small ones and settle as though in a homogeneous liquid of higher viscosity and density.

(ii) For λ=1.16 (mixture number 5), on the other hand, no segregation occurs. Only one shock front is observed at all concentrations whatever be the proportion of small and large particles. This was also observed in Ref. 13 for λ<1.19. We attribute this to the polydispersity of the two size distributions which overlap each other, thus leading to a single-size distribution.

D. Comparison with previous studies

To our knowledge, previous experiments[14–20] on semidilute and concentrated bidisperse suspensions report only on the velocities of the two shock fronts U_{t1} and U_{t2}. Here, c_{s1} is only deduced (never measured) from monodisperse settling velocity, generally reduced to its Richardson–Zaki correlation exponent. Furthermore, $v_s(c_{s0},c_{l0})$ is not inferred from the data, but for the sake of modeling, it is guessed using mainly an extension of the monodisperse theory to the bidisperse case, then, using this guess of $v_s(c_{s0},c_{l0})$ and Eq. (2), the two front velocities are deduced and compared with experiments. Except for recent experiments,[14] the fit looks quite good, but it is rather insensitive and due to the small amount of data (generally five) it cannot cover the whole range of concentrations. To compare our data, we shall consider three items, namely the range of occurrence of segregation process and the velocities of the large and the small particles, $v_l(c_{s0},c_{l0})$ and $v_s(c_{s0},c_{l0})$, respectively.

The most complete previous set of data addressing the issue of segregation occurrence can be found in Davies.[17] There, the measured particle size distribution is of the same order as in ours ($\sigma/a\sim5\%$). Monodisperse settling velocities of each species are given, but not the Stokes velocities. In the experiments, large particles are successively added to small ones (c_{s0}=10%–15%). For λ=2.85 and 2.33, segregation is always observed even up to total concentration c_0 of 50 and 55% in full agreement with our results for λ=2.85 (Fig. 11). For λ=1.69 and c_{s0}=15%, the suspension falls *en masse*, above a total concentration of 41.3%, the two fronts merging into a single one (Fig. 6 of Ref. 17). Large and small particles are interlocked and fall at the same velocity which lies in between that of small and large ones at the same concentration c_0. Our results (Fig. 10, c_I<45%) are in good agreement with these values. Davies' data at λ=1.3 also confirm the trend of the inhibition of segregation at a lower concentration (36%), as the size ratio decreases. Such an interlocked sedimentation can be also found in extrapolating to high concentrations the data of Smith[20] and Smith *et al.*[15] (Fig. 7 of Ref. 15), Lockett and Al-Habbooby[18] (Figs. 17 and 18, although here c_{s0} is small), Al-Naafa and Selim (Fig. 17 of Ref. 14), and even Mirza and Richardson (Figs. 8 and 9 of Ref. 19) who claim that segregation occurs.

The large-particle velocity $v_l(c_{s0},c_{l0})$ (front speed U_{t2}) is in principle easy to compare with the monodisperse case $v_l(c_0,0)$, but due to the different quantities plotted used by different authors (absolute values without Stokes velocity,[17] hindrance function for one and absolute value for the other,[14] or just a Richardson–Zaki fit), comparisons are difficult. Nonetheless, we can find a confirmation of our small and large concentration regimes (see above points 1–3) in Figs. 17 and 18 of Ref. 14 and in Fig. 20 of Ref. 18. For the most complete set of data (Fig. 17 of Ref. 20), with λ~1.9, we have compared, in Fig. 13, the two hindrance functions, they look the same with ours, but we note that the small particle concentration is only 7.88% and that the suspension is colloidal. As noted in the Sec. II, the deduction of $v_s(c_{s0},c_{l0})$ in such studies is difficult because of the lack of a direct measurement of c_{s1}. Various tentative tests we performed on the data sets of Refs. 14–20) leads to values with more than 100% uncertainly even if we assume that the data are quite accurate. Such an example is given in our Fig. 13 with the data of Ref. 15. We reiterate that the accurate determination of $v_s(c_{s0},c_{l0})$ requires measurements, rather than simply an analytical fit, not only of c_{s1} but also of $v_s(c_{s1})$ over the entire range of concentration. While the sedimentation scenario of bidisperse suspensions, as well as the segregation inhibition (17), have already been observed previously,[12–20] this is the first time to our knowledge that the semidilute and concentrated regimes have been described in comparison with monodisperse hindered settling functions. As presented,

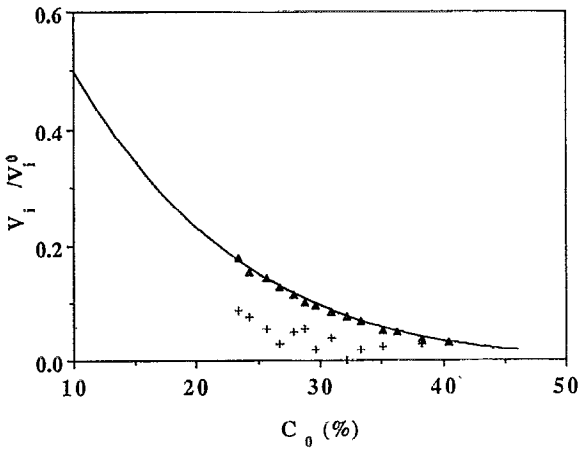

FIG. 13. From Al-Naafa and Selim (14): Normalized sedimentation velocities, for $\lambda=1.68$ and $c_{s0}=7.88\%$. The full line is their monodisperse hindered settling function. Crosses and triangles correspond, respectively, to small and large particles.

our data are suitable for further theoretical interpretations.[32,33]

V. CONCLUSIONS

We have measured the concentration profiles occurring during sedimentation of noncolloidal suspensions of bidisperse glass beads in a Newtonian fluid. From the shape of the profiles, we have derived the sedimentation velocities of both size particles for different size ratios and relative initial particles concentrations. Comparison of the hindered settling functions clearly separate a regime extending the dilute one from a concentrated regime. In the former, large particles hinder more than small particles. For a sufficiently small size ratio, at high concentrations, compared to the respective monodisperse suspensions, large particles are slowed down whereas small ones are dragged along. This ultimately leads to the fading of size segregation. For the particular size ratio of $\lambda=1.68$, this happens at a total concentration around 45%.

ACKNOWLEDGMENTS

This paper has benefited from stimulating discussions with Professors J. C. Bacri, J. Brady, J. Hinch, G. Homsy, R. Jullien and from one referee's suggestions of a better way to present the data. J. M. and D. S. would like to acknowledge support by GDR CNRS Physique des Milieux Hétérogènes complexes.

[1]J. Z. Xue, E. Herbolzheimer, M. A. Rutgers, W. B. Russel, and P. M Chaikin, "Diffusion, dispersion in settling of hard spheres," Phys. Rev. Lett. **69**, 1715 (1992), and references therein.
[2]G. K. Batchelor, "Sedimentation in a dilute dispersion of spheres," J. Fluid Mech. **52**, 245 (1972).
[3]G. J. Kynch, "Theory of sedimentation," Trans. Faraday Soc. **48**, 166 (1952).
[4]J. F. Richardson and W. N. Zaki, "Sedimentation and fluidization: part 1," Trans. Inst. Chem. Eng. **32**, 35 (1954).
[5]J. Happel, "Viscous flow in multiparticle system: slow motion of fluids relative to bed of spherical particles," AIChE J. **4**, 197 (1958).
[6]P. Mazur and W. van Saarloos, "Many-sphere hydrodynamic interactions and mobilities in a suspension," Physica A **115**, 21 (1982).
[7]R. J. Philips, J. Brady, and G. Bossis, "Hydrodynamic transport properties of hard-sphere dispersions. I. Suspensions of freely mobile particles," Phys. Fluids **31**, 3462 (1988).
[8]B. Noetinger, "Sedimentation et transport de particules dans un fluide visqueux," Thèse de Doctorat, Université Pierre et Marie Curie, 1989 (unpublished).
[9]A. J. C. Ladd, "Dynamical simulations of sedimenting spheres," Phys. Fluids A **5**, 299 (1993), and references therein.
[10]G. K. Batchelor, "Sedimentation in a dilute polydisperse system of interacting spheres Part 1 General theory," J. Fluid Mech. **119**, 379 (1982).
[11]G. K. Batchelor and C.-S. Wen, "Sedimentation in a dilute polydisperse system of interacting spheres. Part 2. Numerical results," J. Fluid Mech. **124**, 495 (1982).
[12]R. H. Davis and K. H. Birdsell, "Hindered settling of semidilute monodisperse and polydisperse suspensions," AIChE J. **34**, 123 (1988).
[13]D. Bruneau, R. Anthore, F. Feuillebois, X. Aubray, and C. Petitpas, "Measurements of the average velocity of sedimentation in a dilute polydisperse suspension of spheres," J. Fluid Mech. **119**, 577 (1991).
[14]M. A. Al-Naafa and M. S. Selim, "Sedimentation of monodisperse and bidisperse hard-sphere colloidal suspensions," AIChE J. **38**, 1618 (1992).
[15]T. N. Smith, "The differential sedimentation of particles of two different species," Trans. Inst. Chem. Eng. **43**, 769 (1965), "The sedimentation of particles having dispersion of sizes," *ibid.* **44**, T153 (1966); "The differential sedimentation of particles of various species," *ibid.* **45**, T311 (1967).
[16]R. L. Withmore, "The sedimentation of suspensions of spheres," Br. J. Appl. Phys. **6**, 45 (1955).
[17]R. Davies, "The experimental study of the differential settling of particles in suspension at high concentration," Powder Tech. **2**, 43 (1968).
[18]J. Lockett and H. M. Al-Habbooby, "Differential settling by size of two particle species in a liquid," Trans. Inst. Chem. Eng. **51**, 281 (1973).
[19]S. Mirza and J. F. Richardson, "Sedimentation of suspensions of particles of two or more sizes," Chem. Eng. Sci. **34**, 447 (1979).
[20]M. S. Selim, A. C. Kothari, and R. M. Turian, "Sedimentation of multisized particles in concentrated suspensions," AIChE J. **29**, 1029 (1983).
[21]S. Lee, Y. Jang, C. Choi, and T. Lee, "Combined effect of sedimentation velocity fluctuation and self-sharpening on interface broadening," Phys. Fluids A **4**, 2601 (1992).
[22]J-C. Bacri, M. Hoyos, N. Rakotomalala, D. Salin, M. Bourlion, G. Daccord, R. Lenormand, and A. Soucemarianadin, "Ultrasonic diagnostic in porous media and suspensions," J. Phys. (France) III **1**, 1455 (1991).
[23]J-C. Bacri, C. Leygnac, and D. Salin, "Evidence of capillary hyperdiffusion in two phases flow in porous media," J. Phys. Lett. **46**, I-467 (1985).
[24]J-C. Bacri, D. Salin, and R. Woumeni, "Three-dimensional miscible viscous fingering in porous media," Phys. Rev. Lett. **67**, 2005 (1991).
[25]J-C. Bacri, C. Frenois, M. Hoyos, R. Perzynski, N. Rakotomalala, and D. Salin, "Acoustic study of suspension sedimentation," Europhys. Lett. **2**, 123 (1986).
[26]R. H. Davis and M. A. Hassen, "Spreading of the interface at the top of a slightly polydisperse sedimenting suspension," J. Fluid Mech. **196**, 107 (1988).
[27]M. Hoyos, "Etude des suspensions par acoustique: sédimentation et viscosité," Thèse de Doctorat, Université Paris VII, 1989 (unpublished).
[28]J. Martin, N. Rakotomalala, and D. Salin, "Hydrodynamic dispersion broadening of sedimentation front," to appear in Phys. Fluids.
[29]J. M. Hovem and G. D. Ingram, "Viscous attenuation of sound in saturated sand," J. Acoust. Soc. Am. **66**, 1807 (1974).
[30]M. A. Biot, "Theory of propagation of elastic waves in a fluid saturated porous medium," J. Acoust. Soc. Am. **28**, 168 (1956).
[31]D. Salin and W. Schön, "Acoustic of water saturated packed glass spheres," J. Phys. Lett. **42**, L-477 (1981).
[32]J. Brady and L. Durlofsky, "The sedimentation rate of disordered suspensions," Phys. Fluids **31**, 717 (1988).
[33]A. J. C. Ladd, "Hydrodynamic transport coefficient of random dispersion of hard spheres," J. Chem. Phys. **93**, 3484 (1990).